Crystalline potassium perrhenate: a study using molecular dynamics and lattice dynamics

Crystalline potassium perrhenate: a study using molecular dynamics and lattice dynamics

R J C Brown†§, R M Lynden-Bell†, I R McDonald† and M T Dove‡

† University Chemical Laboratory, University of Cambridge, Lensfield Road, Cambridge CB2 1EW, UK
‡ Mineral Physics Group, Department of Earth Sciences, University of Cambridge, Downing Street, Cambridge CB2 3EQ, UK

Abstract. Molecular dynamics and lattice dynamics calculations have been used to study crystalline $KReO_4$ which has the tetragonal scheelite structure. The charge distribution on the anion and repulsive potential parameters were adjusted to fit the unit cell dimensions at low temperature and zero stress, and were then used to study the properties of the salt over a range of temperature. The results agree satisfactorily with experimental crystallographic and other data over a range of temperature.

1. Introduction

Potassium perrhenate, $KReO_4$, is an ionic crystal with the tetragonal scheelite structure. There are many salts with tetrahedral anions which crystallize in this structure, including most of the alkali metal perrhenates and metaperiodates and the ammonium salts NH_4ReO_4, NH_4TcO_4 and NH_4IO_4. While the potassium salts show no anomalies in their properties as the temperature is raised, the ammonium salts behave in an unusual manner; anomalies have been found in their thermal expansion, thermodynamic and spectroscopic properties, which must be ascribed to the presence of ammonium ions in place of alkali metal ions.

We are embarking on a study of the perrhenates with the aim of investigating the microscopic basis of the anomalous temperature dependence of the properties of ammonium perrhenate. In order to do this we must construct a potential model which gives the correct macroscopic behaviour. It is hoped that the potential function obtained in this way will be useful in describing the interaction between the ammonium ion and other oxyanions. The scheelite structure has a tetragonal unit cell, and the orientation of the anion in the unit cell is not fixed by symmetry. The independent crystallographic parameters are known over a range of temperature, and are sufficient in number to determine the parameters of the potential energy function to be used in molecular dynamics simulations and lattice dynamics calculations. As a first step towards studying the ammonium salt, we construct a model for $KReO_4$ and verify that it gives the correct, albeit unremarkable, behaviour for its properties as functions of temperature. This is the work described in this paper. We shall then use the parameters for the potential function for the potassium salt as the basis for constructing a potential function to describe the ammonium salt, and use this to investigate the microscopic basis of the anomalous behaviour of the latter.

§ On leave from Chemistry Department, Queen's University, Kingston, Ontario K7L 3N6, Canada.

KReO$_4$ crystallizes in the tetragonal scheelite structure, part of which is shown in figure 1; the space group is $I4_1/a$ (No 88). The crystal structure has recently been determined by powder neutron diffraction at three temperatures [1], and references to earlier structure determinations are to be found in that paper. The crystal consists of monatomic K$^+$ cations, and ReO$_4^-$ anions which are only slightly distorted from a regular tetrahedron. The K and Re atoms are situated at the symmetry-determined Wyckoff b and a positions respectively. The three O-atom position coordinates determine the Re–O bond length, the O–Re–O bond angle, and the angle β which defines the anion orientation relative to the unit cell vectors. The fractional coordinates of the atoms in the unit cell were taken with the same origin and definitions as in [1].
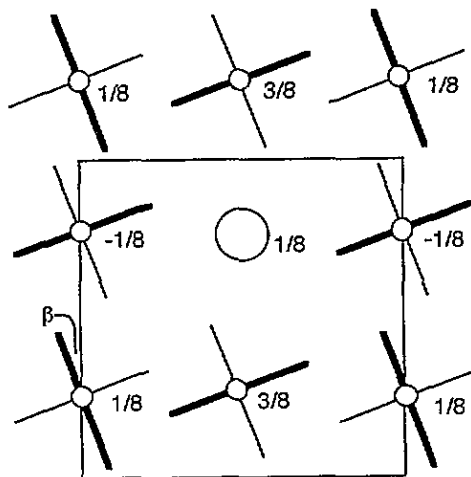

Figure 1. Three layers of the structure of KReO$_4$ as viewed down the c axis. The tetrahedral anions are shown with thicker lines for the Re–O bonds pointing upwards, and thinner lines for the bonds pointing downwards. The K$^+$ ion is shown as a circle. The z fractional coordinates for the K and Re atoms are indicated, and the square base of the unit cell with its origin at an inversion centre is shown.

The thermodynamic properties of crystalline KReO$_4$ and its component ions in the gas phase have been reported, so the molar lattice energy can be calculated readily and compared with the results of the MD calculation. The enthalpy of formation of K$^+$ (g) is +514.007 kJ mol^{-1} [2], of ReO$_4^-$ (g) is −976±30 kJ mol^{-1} [3] and of KReO$_4$ (s) is −1108±15 kJ mol^{-1} [4]. From these data the molar lattice energy of KReO$_4$ is calculated to be −646±33 kJ mol^{-1}. The molar heat capacity has been measured from 15 K up to room temperature and has been accounted for satisfactorily using vibrational frequencies derived from Raman spectroscopy [5, 6].

Lattice mode frequencies of KReO$_4$ (s) have been determined over a wide range of temperature from Raman spectra [7–10]; the IR spectrum has also been reported [11] but gives limited information about the low-frequency modes. Comparison of the experimental lattice mode frequencies with the results of the lattice dynamics calculation provides a stringent test of the potential energy function assumed.

2. Molecular dynamics simulations

Computer simulations were carried out using the method of molecular dynamics [12]. The program was the same as used previously [13, 14] and was run under conditions of constant temperature using a Nosé thermostat, and either constant unit cell dimensions (usually described for simplicity as 'constant volume') or constant pressure using a Parrinello–Rahman barostat. Calculations were carried out on a block of $4 \times 4 \times 2$ unit cells containing a total of 768 atoms. Both constant-volume and constant-pressure calculations were performed and gave essentially the same results. The tetragonal symmetry of the unit cell was stable in all the constant-pressure runs. The timestep used was 0.005 ps and the cut-off for short-range forces was 10 Å. The stresses, the total energy and the orientation of the anion in the unit cell, which is specified by the angle β, were monitored during each run.

The anions were assumed to be rigid regular tetrahedra with a bond length equal to the experimental bond length of 1.739 Å at 15 K [1]. The net charge on the anion was $-e$.

The potential function between atoms was taken as a Born–Mayer potential without any term for the dispersion energy. The potential energy for the interaction between atoms of types i and j separated by a distance r_{ij} was assumed to be

$$V_{ij} = q_i q_j / r_{ij} + A_{ij} \exp\left(-\rho_{ij} r_{ij}\right).$$

The parameters q_i, A_{ij} and ρ_{ij} were chosen so as to bring to zero the two independent diagonal elements of the stress tensor ($\sigma_{xx} = \sigma_{yy}$ and σ_{zz}), calculated at a temperature of 15 K and at constant volume, with the unit cell dimensions fixed equal to their experimental values at this temperature. At such a low temperature the calculated stresses reflect primarily the interionic potential with little contribution from the thermal motion of the ions.

The O–O potential parameters were derived from unpublished calculations on alkali metal sulphates, and were held constant. The K–K repulsion has practically no effect on the results, and its inclusion is largely a formality. The Re atom was assumed to be buried inside the anion and was ignored in calculating the repulsive energy. In seeking a zero stress tensor, two parameters must be adjusted and these were the O-atom charge q_O, which defines the charge distribution within the anion, and one of the O–K repulsive potential parameters, A_{K-O}. It was found that the main effect of changes in q_O was to change the difference in stresses $\sigma_{xx} - \sigma_{zz}$, while changes in A_{K-O} mainly affect the mean stress $(2\sigma_{xx} + \sigma_{zz})/3$. The two independent stress components could fairly readily be brought to zero within 0.05 kbar for runs with constant unit cell geometry, requiring adjustment of q_O to an accuracy of about $+0.0005e$, and of A_{K-O} to an accuracy of about $+200$ kJ mol^{-1}. No consideration was given to the anion orientation (i.e. the angle β) in selecting the potential function parameters. The potential function parameters obtained in this way and used in the simulations are listed in table 1.

Table 1. Potential function parameters.

Repulsive potential:	A_{ij}/kJ mol^{-1}	ρ_{ij}/Å^{-1}
O–O	2.34×10^5	4.18
O–K	1.6197×10^5	3.5735
K–K	1.51×10^5	2.967
Charge distribution within anion: $q_O = -0.582e$ $q_{Re} = 1.328e$.		

After equilibration runs with the potential function parameters chosen as above, constant-volume runs of 2000 steps were carried out at nominal temperatures of 15 K, 150 K

and 298 K, the temperatures at which crystallographic data are available [1]. At the two
higher temperatures, the cell dimensions were changed as required to bring the stress tensor
components close to zero. Constant-pressure runs at a pressure of 1 bar were then carried
out at the same three temperatures, with results which were very similar to the zero-stress
runs at constant volume. The dependences of the average values of a, c, β and the total
energy on temperature are shown in table 2. Computational uncertainties may be judged
from comparison of the runs at constant pressure and constant unit cell dimensions. The pair
distribution functions for the O–K and O–O distances are shown in figure 2 for temperatures
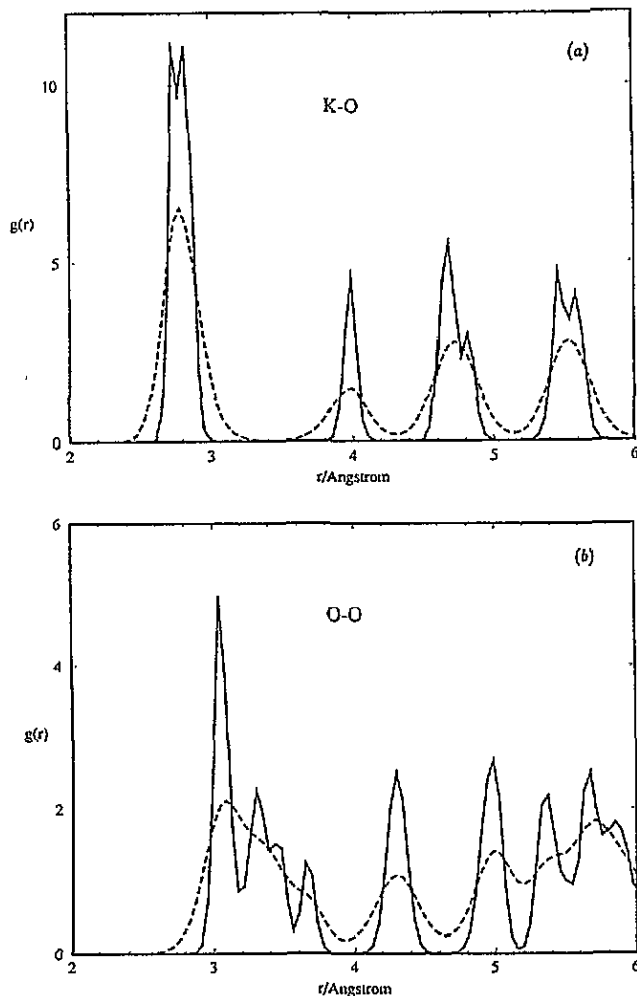of 15 K and 150 K.

Figure 2. (*a*) The radial distribution function for the K–O distance at 15 K (solid line) and
150 K (dashed line). Note the split first peak, and the effect of thermal motion at the higher
temperature on this peak. The integral of the first peak is 2.00, which corresponds to a total of
8.00 oxygen atoms around each cation. (*b*) The radial distribution function for the O–O distance
at 15 K (solid line) and 150 K (dashed line). Atoms in the same anion are not included.

Table 2. Results of the MD calculations. The lattice parameters are reproducible to approximately ±0.1% and the lattice energies to ±0.05 kJ mol⁻¹.

$\langle T\rangle$/K	a/Å	c/Å	β/deg	Lattice energy/ kJ mol⁻¹
Constant volume:				
16.7	5.650	12.556	29.1	−599.57
153.6	5.682	12.657	28.1	−589.24
297.9	5.722	12.800	26.5	−577.51
Constant pressure:				
15.3	5.648	12.53	29.3	−600.00
149.6	5.690	12.64	28.0	−589.37
298.2	5.731	12.77	26.6	−577.56

3. Lattice dynamics calculations

Lattice dynamics calculations were performed using the standard methods within the harmonic approximation, using rigid ions and the same interionic potential as used in the molecular dynamics simulations. The programs used in this work were part of the THB suite of programs as described, for example, by Winkler *et al* [15]. As a preliminary to the lattice dynamics calculation, the equilibrium structure corresponding to the minimum lattice energy was found using a standard program. The rigidity of the ReO_4^- tetrahedron was controlled using a short-range Re–O harmonic potential and a harmonic O–Re–O bond-bending potential with force constants chosen to ensure that the internal mode frequencies would be much larger than the lattice mode frequencies so that the internal and lattice mode vibrations would be decoupled. The remaining harmonic interatomic force constants were formed from the interatomic potentials at the relaxed interatomic distances. Zone-centre frequencies for the lattice modes with their assignments are listed in table 3 and the dispersion curves are shown in figure 3. Elastic constants were also calculated from the lattice energy minimization, and these are given in table 4.

Table 3. Lattice frequencies at the zone centre. T = translational, R = librational modes.

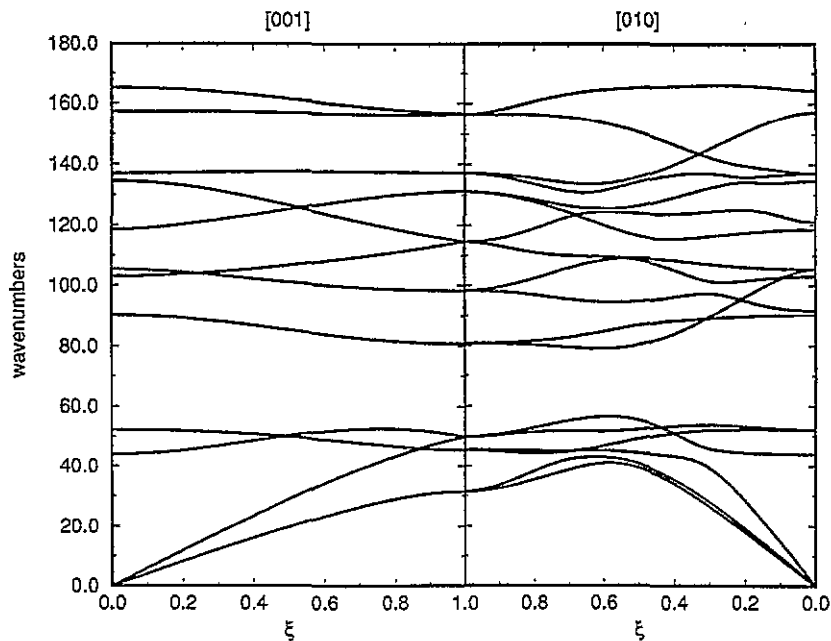| Assignment	Symmetry	Frequency/cm⁻¹	
		Calculated	Observed
Anion T_z	B_g	43.9	59
Anion $T_{x,y}$	E_g	52.1	75
Anion $R_{x,y}$	E_u	91	
Anion R_z	A_g	103.1	115
Cation $T_{x,y}$ + anion $R_{x,y}$	E_g	105.4	132
$T_{x,y}$ optical	E_u	118.6	
T_z optical	A_u	121.1	
Anion R_z	B_u	134.6	
Anion $R_{x,y}$ + cation $T_{x,y}$		137.1	151
Cation T_z	B_g	157.4	160
LO ($k \parallel 001$)	A_u	165.1	

Figure 3. Dispersion curves of lattice frequencies as functions of the reduced wavevector for the external and acoustic mode propagating along the [001] and [010] directions.

Table 4. Calculated elastic constants (units: GPa). Note: $c_{11} = c_{22}$, $c_{44} = c_{55}$, $c_{13} = c_{23}$, $c_{16} = -c_{26}$, and other components are zero.

c_{11}	c_{33}	c_{44}	c_{66}	c_{12}	c_{13}	c_{16}
31.5	23.7	11.4	13.7	12.6	8.3	−1.0

4. Results and discussion

The results of the calculations may be tested by comparison with several experimental data which were not used in setting the potential function parameters: (i) the angle β at 15 K; (ii) the changes in a, c and β with temperature; (iii) the lattice energy; and (iv) the vibrational spectra. The results of the molecular dynamics calculations are shown in table 2. The angle β (see figure 1) was not used fitting the potential function, and so its value at 15 K and its temperature dependence may be used as a test of the potential function. The calculated value of β at 15 K is in excellent agreement with experiment [1], and the changes in a, c and β with temperature are qualitatively correct although somewhat too large. The calculated lattice energy, to which no zero-point energy corrections were applied, is within 8% of the experimental lattice enthalpy, which itself has an uncertainty of 5%.

In the scheelite structure, each cation has two sets of four oxygen atoms nearby. All the oxygen atoms are crystallographically equivalent, but in relation to a particular cation, the two sets are known as the equatorial and axial oxygen atoms. Figure 1 shows part of the structure around a potassium ion viewed down the c axis. The perrhenate tetrahedra have one S_4 axis parallel to the c axis and have inverted configurations in alternate layers. For the particular potassium ion shown, the equatorial oxygen atoms belong to the four tetrahedra in the same plane which are at the corners of the figure, while the axial oxygen

atoms are the closest oxygen atoms on the two nearby tetrahedra in each of the plane above (middle of the top and bottom of the figure) and below (middle of the sides). One can see from this figure that the angle β by which the tetrahedra are twisted is determined by a balance of the K–O attractive forces, and the K–O and O–O repulsive forces.

The radial distribution function for the K–O distance is shown in figure 2(*a*). The first two overlapping peaks at 2.739 Å and 2.825 Å correspond to the different distances from the K atom to the axial and equatorial oxygen atoms; the experimental K–O near-neighbour distances are 2.752 Å and 2.830 Å [1]. The integral of these two peaks is equivalent to a total of 8.00 oxygen atoms adjacent to each potassium atom, as expected [16]. It is notable that at 150 K and higher temperatures, the distinction between these two peaks is smeared out by thermal motion.

The O–O radial distribution function is shown in figure 2(*b*). At a temperature of 15 K, the first peak occurs at 3.055 Å for the O–O nearest-neighbour distance [1]; together with the agreement between the calculated and experimental values of β, this suggests that the parameters for the repulsive potential for the K–O and O–O interactions are satisfactory. It was confirmed that the anion executes restricted librational motion, and not overall rotation.

The zone centre translational and librational mode frequencies listed in table 3 agree qualitatively with those derived from Raman spectra, although the calculated anion librational frequencies are somewhat too small. The components of the calculated elastic constant tensor are listed in table 4. There are no experimental data for $KReO_4$ with which these may be compared. The values for K_2SO_4 are about 50% higher [17]. However, these numbers may be combined with the two linear thermal expansion coefficients estimated from the lattice constants at 150 K and 298 K to calculate the difference between the constant-stress and constant-strain heat capacities [6], leading to 3.0 J K^{-1} mol^{-1}, which may be compared with the estimate of 4.3 J K^{-1} mol^{-1} derived from the measured heat capacities and the Raman spectra. Figure 3 shows dispersion curves for the external mode frequencies plotted as functions of wavevector in the [010] and [001] directions. The optical mode frequencies show moderate dispersion, and there is a gap between the anion translational modes around 50 cm^{-1} and the higher-frequency modes. The calculated density of states for the external and acoustic modes is shown in figure 4, and was used to calculate the quantum heat capacity, which should be valid for low temperatures at which the internal modes of the anion are not appreciably excited. The calculated low-temperature heat capacity indicates a Debye temperature of 104 K; the revised analysis of the experimental data yielded a value of 94 K [6].

There is consistent evidence that the potential function is somewhat softer than it ought to be. The temperature dependences of the crystallographic parameters is too large, and in the 10–50 K temperature range the calculated heat capacity rises more rapidly than experimental data suggesting that the density of states at low frequencies is too high.

5. Conclusions

These calculations, based upon a simple potential function model including short-range repulsions and electrostatic terms only, provides an adequate model for molecular dynamics simulations of this non-trivial crystal from which a number of properties may be calculated with a fair degree of success. It might be possible to construct a more sophisticated model including polarizability and more interaction sites which gave better agreement with experiment. But our aim is to construct a simple potential which can be calculated rapidly for use in a molecular dynamics simulation, and which can be used for the more complex case of ammonium perrhenate.
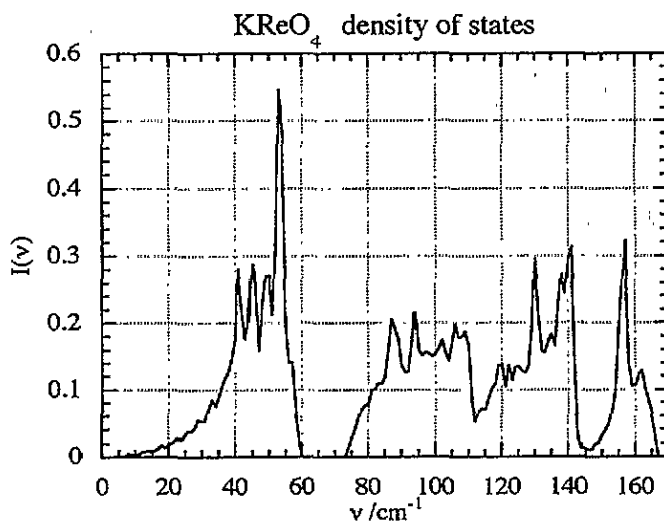
KReO$_4$ density of states

Figure 4. The density of states for the external and acoustic modes, calculated from the dispersion curves shown in figure 3.

Acknowledgments

References

[1] Brown R J C, Powell B M and Stuart S N 1993 *Acta Crystallogr.* C **49** 214
[2] *JANAF Thermochemical Tables* 1985 *J. Phys. Chem. Ref. Data Suppl.* 1 **15** 1407
[3] Sidorov L N, Rudnyi E B, Nikitin M I and Sorokin I D 1983 *Dokl. Akad. Nauk. SSR* **272** 1172
[4] Johnson D A 1990 *J. Chem. Soc. Dalton Trans.* 3301
[5] Weir R D and Staveley L A K 1980 *J. Chem. Phys.* **73** 1386
[6] Brown R J C, Callanan J E, Weir R D and Westrum E F 1986 *J. Chem. Phys.* **85** 5963
[7] Korppi-Tommola J, Brown R J C, Shurvell H F and Sala O 1981 *J. Raman Spectrosc.* **11** 363
[8] Johnson R A, Rogers M T and Leroy G E 1972 *J. Chem. Phys.* **56** 789
[9] Breitinger D K, Emmet L and Kress W 1981 *Ber. Bunsenges. Phys. Chem.* **85** 504
[10] Jayaraman A, Kourouklis G A, Van Uitert L G, Grodkiewicz W H and Maines R G 1988 *Physica* A **156** 325
[11] Muller A 1965 *Z. Naturf.* a **21** 433
[12] Allen M P and Tildesley D J 1987 *Computer Simulation of Liquids* (Oxford: Oxford University Press)
[13] Lynden-Bell R M, Ferrario M, McDonald I R and Salje E 1989 *J. Phys.: Condens. Matter* 1 6523
[14] Ferrario M, Lynden-Bell R M and McDonald I R 1994 *J. Phys.: Condens. Matter* 6 1345
[15] Winkler B, Dove M T and Leslie M 1991 *Am. Mineral.* **76** 313
[16] Szabo A J and Brown R J C 1994 *Z. Naturf.* a **49** 302
[17] Haussuhl S 1965 *Acta Crystallogr.* **18** 839